Electrochimica Acta 83 (2012) 311–320

Contents lists available at SciVerse ScienceDirect

Electrochimica Acta

journal homepage: www.elsevier.com/locate/electacta

One-pot approach to modify nanostructured gold surfaces through in situ dithiocarbamate linkages

I. Almeida [a], V.C. Ferreira [a], M.F. Montemor [b,1], L.M. Abrantes [a,1], A.S. Viana [a,*,1]

[a] Centro de Química e Bioquímica, Departamento de Química e Bioquímica, Faculdade de Ciências da Universidade de Lisboa, Ed. C8, Campo Grande, 1749-016 Lisboa, Portugal
[b] ICEMS, DEQB, Instituto Superior Técnico, Universidade Técnica de Lisboa, Av. Rovisco Pais, 1049-001 Lisboa, Portugal

ARTICLE INFO

Article history:
Received 14 March 2012
Received in revised form 6 August 2012
Accepted 6 August 2012
Available online 13 August 2012

Keywords:
In situ dithiocarbamate modification
Gold nanoparticles
Epinephrine
Tryptophan
Glucose oxidase

ABSTRACT

This work describes a simple methodology to bio-functionalize flat Au(1 1 1) electrodes through the one-step reaction between gold nanoparticles (AuNPs), carbon disulfide and a secondary amine (epinephrine) and an aminoacid (tryptophan). The process relies on the in situ dithiocarbamate formation between carbon disulphide and amine groups and also on the strong linkage between sulfur and gold. The redox behavior of modified gold with epinephrine or tryptophan, prepared from both ethanolic and aqueous solutions confirms their covalent immobilization and reveals a significant increase of their amount on the electrode due to the presence of AuNPs. Electrochemical reductive desorption in basic solution provided qualitative information on the amount of sulfur linked the gold surface and complements the redox studies. The co-immobilization of an enzyme (glucose oxidase, GOx) and gold nanoparticles, using carbon disulfide has been also tested. The presence of GOx on modified Au(1 1 1) electrodes has been confirmed by electrochemical detection of the catalytic oxidation of glucose in the presence of a redox mediator and through the evaluation of H_2O_2 reduction, formed during the catalytic reaction. XPS analysis, topographic and phase imaging by atomic force microscopy (AFM) further confirmed surface modification by AuNPs and also their functionalization. The successful one-step amine adsorption, in the presence of AuNPs, from aqueous solutions reveals the potential of this method in the construction of nanostructured biosensing interfaces.

1. Introduction

Gold nanoparticles have been extensively and successfully used to build tridimensional biosensing interfaces with improved biorecognition sensitivity [1–3]. The large surface/volume ratio allied to the unique optical/electronic properties of nanoparticles is the motors for the increased research in this field. Due to these characteristics AuNPs have a strong adsorption capability and high catalytic efficiencies, and are used as electron transfer mediators to amplify the rate of electron transfer between enzymes and electrodes in biosensors [4–9]. Commonly, the preparation of nanostructured electrodes for catalysis or biosensor applications comprehends several steps, namely (i) gold surface modification with thiols or dithiols derivatives [10]; (ii) incubation with AuNPs; (iii) reaction with a second sulfur derivative containing a suitable terminal group to establish a covalent bond with the catalyst or biomolecule [11,12]; and (iv) one more intermediate activation step with for example EDC/NHS is also required for covalent binding [13].

Recently, the authors have reported [14] that a simple one-pot methodology in the presence of CS_2 could be used for the direct immobilization of glucose oxidase on flat Au(1 1 1) surfaces, with preservation of its biological activity. These results were complemented and supported by the efficient one-step immobilization of either a primary (dopamine) or a secondary (epinephrine) amine, and also an aminoacid (tryptophan). Several studies have demonstrated that in situ formation of a dithiocarbamate through the prompt reaction between carbon disulfide and amines (mainly secondary) [15–18] could be useful for the formation of stable self-assembled monolayers with similar properties of those of thiol derivatives on gold [10]. The main structural feature of dithiocarbamates monolayers is the electron resonance between nitrogen, carbon and sulfur [19,20], which is claimed to be responsible for a strong interaction with the gold substrate, due to an appropriate overlapping of metal and adsorbate molecular orbitals. In addition, it was also demonstrated that in situ dithiocarbamates could be also formed on colloidal gold [15,21,22] and electrodeposited gold nanoparticles [23].

The novelty of the work described here regarding previous studies with thiolated SAMs, or with in situ dithiocarbamates on

* Corresponding author. Tel.: +351 21750000; fax: +351 217500088.
E-mail address: anaviana@fc.ul.pt (A.S. Viana).
[1] ISE member.

0013-4686/$ – see front matter © 2012 Elsevier Ltd. All rights reserved.
http://dx.doi.org/10.1016/j.electacta.2012.08.021

gold, is the simple one-pot methodology, in ethanolic or aqueous solutions, employed to build nanostructured electrodes, involving CS_2, AuNPs (with ca. 22 nm diameter) and compounds containing amines (epinephrine and tryptophan). Glucose oxidase was the enzyme chosen to reveal the potential of this simple method to immobilize biomolecules from aqueous medium. The modification of AuNPs was investigated by UV–vis spectroscopy and atomic force microscopy (AFM) on mica surfaces. Epinephrine and tryptophan covalent attachment has been confirmed through their redox behavior and XPS analysis, while the biological activity of immobilized GOx was evaluated toward glucose oxidation. AFM imaging of gold modified electrodes further confirmed the presence of functionalized AuNPs.

2. Experimental

2.1. Chemicals

Carbon disulfide (Acros Organics), epinephrine (Sigma–Aldrich), tryptophan (Sigma–Aldrich), $HAuCl_4{\cdot}2H_2O$, sodium citrate (Alfa Aesar), sodium hydroxide (Fluka), sulfuric acid (Pancreac), phosphate buffer saline (PBS) (8.0 mM Na_2PO_4 (Merck); 1.14 mM KH_2PO_4 (Merck); 138 mM NaCl (Merck) and 2.7 mM KCl (Merck); pH 6.8) and absolute ethanol (Riedel-de Häen) were all analytical grade and used without further purification. Glucose oxidase from *Aspergillus niger* (GOx, Type X–S, lyophilized powder, 100,000–250,000 units/g, Sigma–Aldrich) was also used without further purification procedure, D(+)glucose from Merck and ferrocenedicarboxylic acid were obtained from Sigma–Aldrich. Glucose solution was allowed to come to mutarotation before its employment, which was prepared in PBS (pH 6.8) and left at 4 °C overnight to allow the equilibration of the anomers. Ultrapure water was obtained from a MILLI-Q A10 Gradient purification system (18 MΩ cm at 25 °C) and used to prepare all the aqueous solutions.

2.2. Thin layer gold electrodes and nanoparticle synthesis

The substrate used for monolayer preparation was a gold film (200 nm) deposited on borosilicate glass (pre-layer of chromium, 2–4 nm) from Arrandee™. The surface was cleaned with *piranha* solution (3:1 mixture (v/v) of H_2SO_4:H_2O_2), rinsed with ultra-pure water and ethanol, and flame annealed, leading to a predominant (1 1 1) crystallographic orientation and a surface roughness of 1.2. The morphologic characterization of bare gold surfaces has been previously described [14,24]. The citrate-stabilized gold nanoparticles (AuNPs/citrate) were synthesized by the Turkevich method [25,26], using 5.0 μmol $HAuCl_4$ in 19 mL of boiling water and 2 mL of 0.5% sodium citrate, prepared according to the procedure previously reported [27]. The colloidal suspensions were characterized by TEM [27], UV–vis and AFM, and stored in the dark at 4 °C. Modification of synthesized AuNPs/citrate in the colloidal suspension with CS_2, CS_2/epinephrine, CS_2/tryptophan and CS_2/glucose oxidase was performed by mixing 250 μL of colloidal suspension with 0.5 mM of CS_2 and 0.50 mM epinephrine/tryptophan and 0.50 mM CS_2/GOx (0.1 mg/ml).

2.3. Electrode modification

Au(1 1 1) electrodes have been modified using one-step method. Au in contact with a mixture of (i) AuNPs/citrate (4 nM), CS_2 (1 mM) and epinephrine or tryptophan (0.1 M) in ethanol or aqueous solutions, during 16 h (RT, 22 °C); and (ii) AuNPs/citrate (4 nM) with CS_2 (1 mM) and glucose oxidase (1 mg/mL) during 16 h, in aqueous solution at 4 °C. The AuNPs concentration was chosen based on a previous study [27] concerning Au(1 1 1) modification with consecutive layers of dithiols and nanoparticles. The flat gold electrodes were also modified by reaction between CS_2 (0.1 M) and epinephrine or tryptophan (0.1 M) in ethanol or aqueous solution, during 16 h, at room temperature. Following the immobilization, the electrodes were thoroughly washed with ultra-pure water, in order to remove any physically adsorbed particles, and dried under a nitrogen flow.

2.4. Electrochemical measurements

Cyclic voltammetry was performed using a PARSTAT 2263 electrochemical work station (Perkin Elmer). A one-compartment Teflon cell was employed, fitted with a saturated calomel electrode (SCE) and a platinum foil, as reference and counter-electrode, respectively. The geometric area of the working electrode (0.57 cm^2) was defined by an O-ring. The electrolyte solutions were degassed for at least 20 min, with nitrogen (99.99997%) prior to each experiment.

2.5. XPS characterization

XPS analysis were carried out using a Microlab 310 F (Thermo Electron-former VG Scientific) with a Mg (monochromated) anode, a concentric hemispherical analyzer and was operated at under pressures lower than 5×10^{-9} mbar, using an Al radiation (monochromator). The XP spectra were obtained in CAE mode (30 eV) and accelerating voltage of 15 kV. The peak quantification was determined after fitting, using a Gaussian–Lorentzian product function and the algorithm was based on the Simplex optimization (Avantage software).

2.6. Morphological characterization

The morphology of modified electrodes with AuNPs was characterized by Tapping mode AFM, in ambient conditions, using a Nanoscope IIIa Multimode AFM (Digital Instruments, Veeco), and etched silicon tips (~300 kHz). Images of AuNPs/citrate before and after modification in colloidal suspension were acquired by placing a drop of the colloidal suspension onto freshly cleaved mica for 15 min, rinsing with water and drying with pure N_2.

3. Results and discussion

3.1. One-step immobilization of in situ dithiocarbamates/AuNPs on Au(1 1 1)

Fig. 1a and b shows, respectively, the cyclic voltammograms obtained upon the reaction of epinephrine and tryptophan with CS_2 in ethanol, in the presence of Au(1 1 1) substrate, with or without the addition of AuNPs. Table 1 compiles the electrochemical data obtained from the cyclic voltammograms shown in Fig. 1. The redox response of epinephrine and the linear dependence of both anodic and cathodic peak currents on the sweep rate (inset of Fig. 1a) confirm the stable linkage of epinephrine to the electrode surface and clearly indicate that its redox process is not controlled by diffusion. It is verified that in the presence of AuNPs epinephrine oxidation and reduction peaks are nearly symmetric, with a half-wave potential negatively shifted regarding the one observed for modified Au(1 1 1) in the absence of AuNPs [14], indicating a slight facilitated electron transfer. Surface coverages were estimated based on the integration of the oxidation processes, considering that two electrons are transferred during the reversible electrochemical conversion of the hydroquinone/quinone forms of epinephrine [14,29]. The addition of AuNPs into the reaction resulted in a great increase of epinephrine surface concentration (based on Au (1 1 1) electrode area) from 1.3×10^{-10} to ca. 4.0×10^{-10} mol cm^{-2}, demonstrating

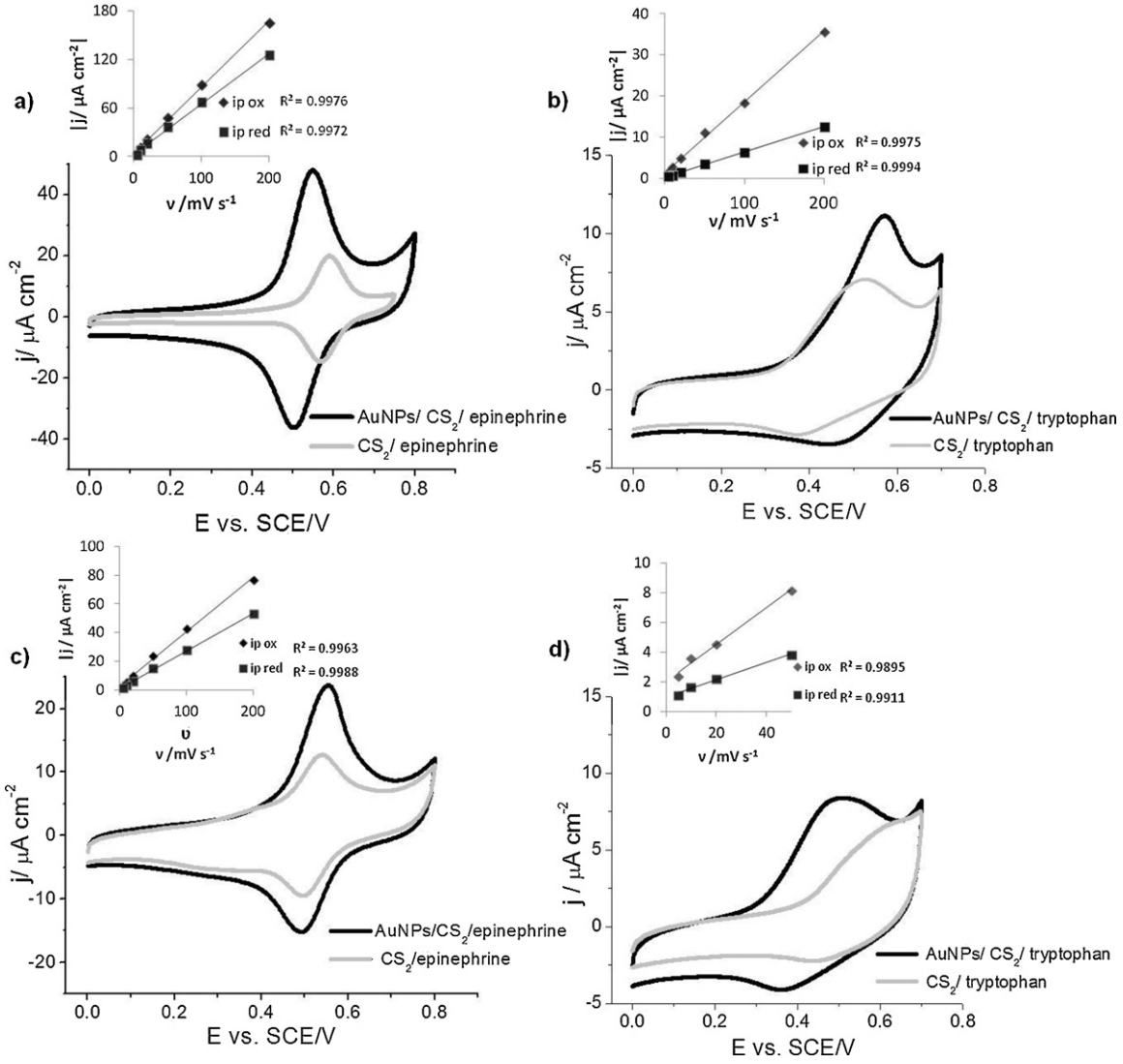

Fig. 1. Cyclic voltammetry of CS_2/epinephrine and CS_2/tryptophan reaction on Au surface, in the presence and absence of AuNPs, from ethanolic (a) and (b) and aqueous (c) and (d) solutions: 0.1 M H_2SO_4, $\nu = 50\,mV\,s^{-1}$. Inset: peak current density vs. scan rate for the modified electrodes in the presence of AuNPs.

the efficiency of this one-step procedure. As discussed in a previous work [14], the redox behavior of tryptophan in solution or immobilized is not straightforward. In most surfaces a single oxidation peak is detected, which is due to an irreversible $2e^-$ reaction with the formation of an extremely reactive methylene–imine intermediate [30–33], giving rise to species that cannot be electrochemically reduced on the reverse scan. This explains the non-symmetrical responses obtained in the cyclic voltammograms of Fig. 1b, which consistently show a much larger oxidation peak than its reduction counterpart. Notwithstanding, the linearity between the peak current and the sweep rate observed for Au/AuNPs/CS_2/tryptophan (Fig. 1b), expected for a non-diffusional controlled electron transfer, confirms the adsorption and stability of the aminoacid on the surface. It is also clear from the surface coverage values presented in Table 1, in similarity with the behavior observed for epinephrine, that more tryptophan molecules (per Au(1 1 1) geometric area) could be immobilized in the presence of AuNPs. The lower coverage obtained for tryptophan modified electrodes regarding those

Table 1
Half-wave potential, $E_{1/2}$, peak potential separation, ΔE_p, and surface coverage, Γ, values obtained from the cyclic voltammograms of modified electrodes shown in Fig. 1.

Modified electrodes	Solvent	$E_{1/2}$ (V)[a]	ΔE_p (V)	Γ^{ox} ($\times 10^{-10}$)/(mol/cm^2)
CS_2/epinephrine	Organic	0.57	0.02	1.3
	Aqueous	0.52	0.05	0.7
AuNPs/CS_2/epinephrine	Organic	0.53	0.05	4.0
	Aqueous	0.52	0.05	2.0
CS_2/trytophan	Organic	0.43	0.14	0.8
	Aqueous	0.52	0.16	0. 3
AuNPs/CS_2/tryptophan	Organic	0.51	0.12	1.1
	Aqueous	0.43	0.15	0.9

[a] Potential vs. SCE.

of epinephrine, must be related with the higher reactivity between secondary amines and carbon disulfide, as reported before [17] and also confirmed in our previous work [14].

Since our main purpose is the direct attachment of biomolecules, which often requires aqueous environments, the one-step immobilization of epinephrine and tryptophan was also tested in buffered aqueous solutions, and the representative voltammograms are presented in Fig. 1c and d, respectively. It can be verified that the attachment of both epinephrine and tryptophan is more effective in ethanolic solutions than in aqueous, probably due to the low solubility of CS_2 in the more polar solvent. Notwithstanding, it is clearly observed, that the presence of nanoparticles leads to a substantial increase in the peak currents for both compounds (Table 1), as verified when the immobilization was performed in ethanolic solutions. The linear relationship between current density and sweep rate was also observed for both modified electrodes, in the presence of AuNPs, however for tryptophan this proportionality is only achieved up to 50 mV s^{-1} (inset of Fig. 1d), which indicates a more complex electron transfer during tryptophan redox process. It is worth noting that the loss of linearity between current and sweep rate for larger potential scan rates is not associated with a loss of immobilized tryptophan molecules, as verified through consecutive potential cycles. Estimated values for electrode coverages (based on geometric area and using the same methodology to integrate ill-defined peaks, such as those of tryptophan) are remarkably higher in the presence of gold nanoparticles, either from ethanolic or aqueous solutions. This amplification effect is a direct consequence of a larger available area for adsorption when the AuNPs are present. The electrochemical data confirm the applicability of this one-pot procedure to adsorb amine compounds, and shows the potential applications on the single-step adsorption of proteins on a gold surface, since they contain a large number of primary and secondary amine groups.

In order to prove the important role of CS_2 on the stability and strong linkage of epinephrine to AuNPs, the 2nd and the 10th cycle of a Au (1 1 1) surface after exposure to ethanolic solutions of CS_2, AuNPs and epinephrine, or to AuNPs and epinephrine have been recorded (Fig. S1a, Supplementary Materials). While in the presence of CS_2 the effect of potential cycling on the redox response of epinephrine is minimum, the same behavior is not true in the absence of CS_2. The low amount of physically adsorbed molecules responsible for the reversible redox process (Fig. S1b, Supplementary Materials) on the 2nd cycle does not preclude the appearance of the characteristic peak for the chromium oxidation on the 10th cycle, arising from the instability of the bare Au/Cr thin layer electrodes after consecutive potential scanning in 0.1 M H_2SO_4. It is worth noting that this process is only detected on bare gold after multiple potential cycling. It is thus obvious that CS_2 is playing a crucial role in the stability of the adsorbed compounds and AuNPs, most probably promoting a covalent bonding between epinephrine and gold surfaces.

The redox behavior discussed in Fig. 1 was complemented with electrochemical reductive desorption studies, commonly used to characterize alkanethiol SAMs on gold, since it can provide relevant information on their organization, packing and stability [24,34,35]. The cyclic voltammograms shown in Fig. 2 correspond to the electrochemical stripping of SAMs formed from only CS_2 or CS_2 and AuNPs, prepared in ethanolic (Fig. 2a) or aqueous (Fig. 2b) solutions, respectively. Fig. 2a shows a single sharp reduction peak at −0.92 V, assigned to desorption of both sulfur atoms of CS_2 from flat Au(1 1 1), while a broader peak at slightly lower potentials (−0.98 V) with a shoulder (−0.89 V) can be denoted in the presence of AuNPs, indicating that distinct sulfur environments coexist in the 3D assembly. When Au(1 1 1) is modified in aqueous solution with nanoparticles and CS_2, a similar conclusion can be withdrawn from the electrochemical data (Fig. 2b), where two obvious stripping peaks can be clearly denoted. Besides, there is also a great increase in the reduction currents and therefore on the amount of sulfur detached from gold when AuNPs are present.

The electrochemical desorption of a cadmium dibutyl dithiocarbamate (dibutylDTC) [36] SAM formed on Au (1 1 1) from ethanolic solution exhibits one major reductive peak (Fig. S2, Supplementary Materials) at the same potential value than that obtained for a pure CS_2 SAM shown in Fig. 2a (Table 2). It is verified that dithiocarbamates of distinct chain lengths, having different organizations on the surface, exhibit peak desorption potentials ranging from −0.75 [14] to −0.92 V, which cover the values obtained in this study for the in situ dithiocarbamates formed on gold (Fig. 3a and b). This indicates that a S_2—C—N resonance structure does not dictate *per se* the stability of monolayers on gold (regarding a CS_2 linkage), since the aliphatic chains or aromatic π–π stacking interactions among adsorbates may impart additional stability to the self-assembled monolayers. The reductive desorption of monolayers formed from the reaction between CS_2 and epinephrine or tryptophan in ethanolic solutions, either in the presence or absence of AuNPs, is shown in Fig. 3a. In all cases the reduction potentials are slightly positively shifted from that of pure CS_2 SAMs, exhibiting broader desorption peaks, which supports the formation of dithiocarbamates on gold. There is a clear increase of the cathodic peak intensity when the electrodes are modified in the presence of AuNPs, as also confirmed through the charge involved in the reduction process, and therefore on the total amount of immobilized sulfur on the gold surface. As depicted from Table 2, sulfur concentration for the modified electrodes without AuNPs (estimated based on the Au(1 1 1) geometric area), assuming the involvement of one electron per each sulfur atom desorbed, are close to those expected for a packed alkylthiol ($\sqrt{3} \times \sqrt{3}$)/R30° overlayer structure at Au (1 1 1), 7.6×10^{-10} mol cm^{-2} [24]. In organic solution, the increase on the amount of adsorbed aminoacid due to the presence of nanoparticles, obtained from its redox response (Table 1) agrees with the augment in sulfur coverage (ca. 25% increase, Table 2). However, for epinephrine modified electrodes with AuNPs, the increase in sulfur surface concentration is considerably smaller than that detected for epinephrine oxidation in the same systems. Electrochemically, the detected sulfur atoms should be the ones directly adsorbed to the flat surface, plus a possible small contribution from sulfur species attached to the AuNPs in the close vicinity of the electrode [37], also reduced during desorption. Taking into account that the presence of AuNPs causes only a small increase in sulfur coverage (Fig. 3a) but a noticeable increase on epinephrine oxidation currents (Fig. 1a), the data indicates that a large part of epinephrine molecules must be stably attached to the AuNPs.

When flat Au(1 1 1) electrodes are modified with tryptophan (Fig. 3b) in aqueous solutions, in the presence of AuNPs, a single and well-defined reduction peak is obtained with a potential value close to those observed for layers prepared in ethanol (Table 2). This indicates that the presence of AuNPs significantly improves the amount of sulfur on the surface (as observed in Fig. 2b), and also of tryptophan molecules in agreement with the voltammetric responses of Fig. 1d and Table 1. This effect is also observed for epinephrine modified electrodes, although the current increase is not as significant, since DTCs are formed in aqueous environment with this compound (containing a secondary amine) in the absence of AuNPs (Fig. 1c). The citrate ions that stabilize the AuNPs are likely to increase the CS_2 solubility in water, near the gold surfaces, promoting the adsorption of sulfur species (CS_2 or DTC).

XPS analysis was performed on Au (1 1 1)/AuNPs/CS_2, Au(1 1 1)/CS_2/epinephrine and Au (1 1 1)/AuNPs/CS_2/epinephrine aiming to characterize the surface bonds established during the one-step modification. Fig. 4 shows the ionization of S2p expected to be present when dithiocarbamates are adsorbed on gold. The S2p ionization for Au(1 1 1)/CS_2/epinephrine and

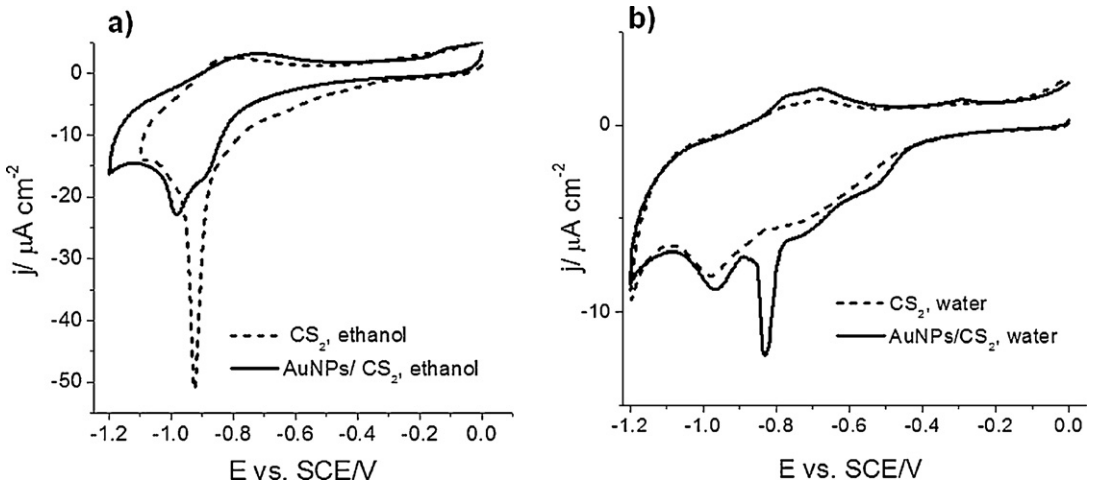

Fig. 2. Cyclic voltammograms of modified gold electrodes with CS_2, in the presence and absence of AuNPs, from ethanol (a) and aqueous (b) solutions: 0.1 M NaOH; $\nu = 20\,mV\,s^{-1}$.

Table 2
Reduction peak potentials, E_p^{red}, and surface coverage values obtained from the cyclic voltammograms of modified electrodes shown in Fig. 3.

Modified electrodes	CS_2		Dibutyl-DTC	CS_2/epinephrine	CS_2/tryptophan		AuNPs/CS_2/epinephrine	AuNPs/CS_2/tryptophan	
	Organic[a]	Aqueous	Aqueous	Organic[a]	Organic[a]	Aqueous	Organic	Organic	Aqueous
E_p^{red} vs. SCE/V	−0.92	−0.70 −0.97	−0.90	−0.90	−0.88	−0.73 −0.96	−0.90	−0.90	−0.8
Γ^{red} ($\times 10^{-10}$)/(mol cm^{-2})[b]	4.3	1.3 1.4	1.7	6.4	5.2	0.7 1.6	8.2	7.0	6.0

[a] Ref. [14].
[b] Total sulfur surface concentration (assuming one electron per each sulfur atom).

Au(1 1 1)/AuNPs/CS_2/epinephrine exhibits one typical metal-sulfur bond (Au-S), characterized by the S2p$_{3/2}$ and S2p$_{1/2}$ doublet with an electron binding energy (BE) of 162.7 eV for S2p$_{3/2}$ (164 eV for Sp$_{1/2}$). The BE values are in agreement to those reported for in situ prepared dithiocarbamates [15,19], slightly higher than those of pure dithiocarbamates (Sp3/2 ~ 162 eV [19]), but still lower than free unbounded thiols or disulfides (ca. 163.7 eV [38,39]). Likewise reported for 2D and 3D (with nanoparticles) short alkanethiolate self-assembled monolayers on gold [40], the S2p BE is almost identical for epinephrine modified electrodes with or without AuNPs. The XP results of Au (1 1 1)/AuNPs/CS_2 also reveal only one sulfur–gold species with a binding energy for S2p$_{3/2}$ of 162.2 eV with the typical spin–orbit separation of 1.2 eV [41]. It is worth to note that neither unbound sulfur nor nitrogen containing species could be detected in this sample. In contrast, both epinephrine samples show N1s ionizations with binding energies of 400.9 eV, which are values close to those reported for C—N bond in DTC SAMs [15,19,42].

Because of the low amount of deposited molecules, the signal to background ratio of the XPS measurements, does not allow an accurate identification of the binding energies for the Au—S bond from DTC or CS_2 in the same sample, or even a possible AuNP—S—C—S—Au(1 1 1) linkage, that could be established in the presence of nanoparticles. Notwithstanding, the qualitative

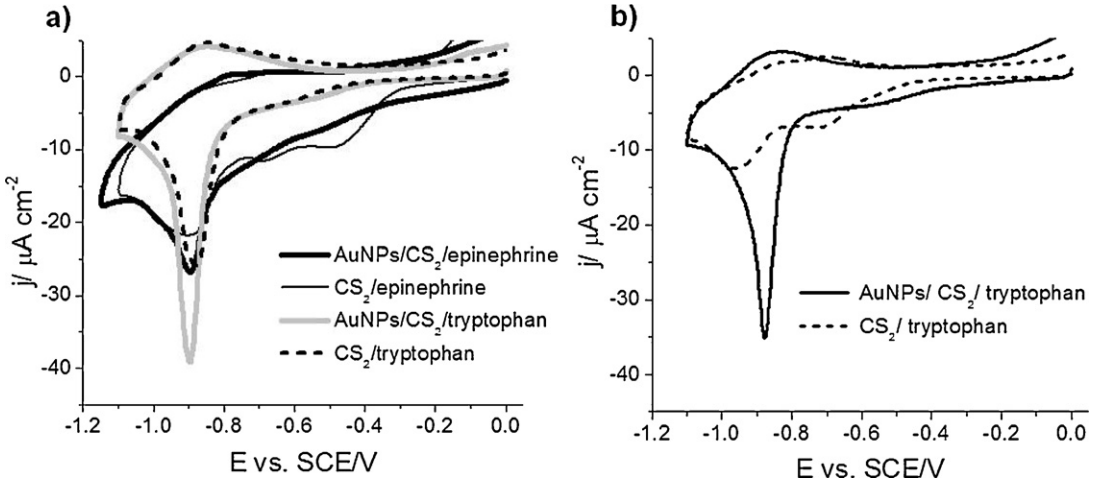

Fig. 3. Cyclic voltammograms of modified gold electrodes with (a) CS_2/epinephrine and CS_2/tryptophan, in the presence and absence of AuNPs, from ethanol; (b) CS_2/tryptophan, in the presence and absence of AuNPs, from aqueous solutions: 0.1 M NaOH; $\nu = 20\,mV\,s^{-1}$.

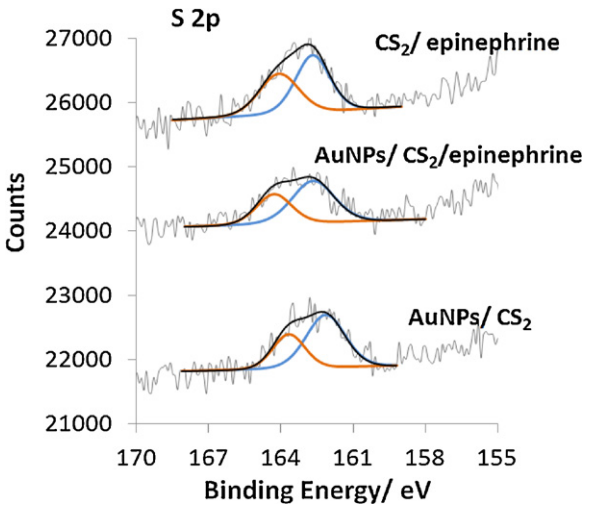

Fig. 4. S2p XPS spectra of modified gold surfaces.

information provided by the binding energies confirm a strong coupling with a covalent character between sulfur and gold surfaces for all studied samples.

The morphology of the modified Au (1 1 1) electrodes upon the reaction between AuNPs, CS_2 and epinephrine (Fig. 5a) from ethanol solutions, or tryptophan from both ethanolic (Fig. 5b) and aqueous (Fig. 5c) medium, were characterized by AFM. Typical gold monoatomic terraces are still visualized together with gold nanoparticles with average diameters of 34 ± 7 nm, 33 ± 6 nm and 30 ± 8 nm, respectively, indicative of functionalization of pristine AuNPs/citrate (with average diameters of 22 ± 6 nm, Fig. 6a) during the deposition process.

Colloidal AuNPs/citrate were modified in a mixture of CS_2 and epinephrine or tryptophan (in the absence of Au (1 1 1) surface) from ethanolic solutions, to assess the in situ dithiocarbamate formation on nanoparticles, and characterized by UV–vis spectroscopy (Fig. S3, Supplementary Materials) and AFM. The topographic images, corresponding profiles and size distribution histograms are presented in Fig. 6. The UV–vis spectrum corresponding to the AuNPs stabilized by citrate ions reveals a characteristic plasmon resonance band centered at 522 nm (Fig. S3, Supplementary Materials) [27], which agrees with the reported behavior for particles with ca. 20 nm of diameter [26–28], corroborating the sizes depicted in Fig. 6a. In contact with only CS_2 the AuNPs tend to form small aggregates (average sizes of 23 ± 6 nm) of undefined shapes (Fig. 6b). However, upon the reaction with CS_2/epinephrine (Fig. 6c) and CS_2/tryptophan (Fig. 6d) there is a significant increase of the average diameters up to 55 ± 13 nm and 60 ± 12 nm, with globular shapes.

It is worth noting that the average diameter of the functionalized AuNPs attached to the gold surface is smaller than those obtained when the reaction takes place in colloidal suspension (Fig. 6) in the absence of Au(1 1 1) electrode, but still larger when compared to the AuNPs/citrate diameters. The very fast reaction between AuNPs, CS_2 and epinephrine or tryptophan, and consequent adsorption to the gold surface should avoid the aggregation of AuNPs. Due to the spontaneity of the one-step methodology, the areas in AFM imaging which are AuNPs free should be covered with CS_2 molecules or by dithiocarbamates formed from the reaction between CS_2 and epinephrine or tryptophan. Once CS_2 molecules are adsorbed on gold, the exposed carbon atoms are no longer reactive toward amine functions in solution. This

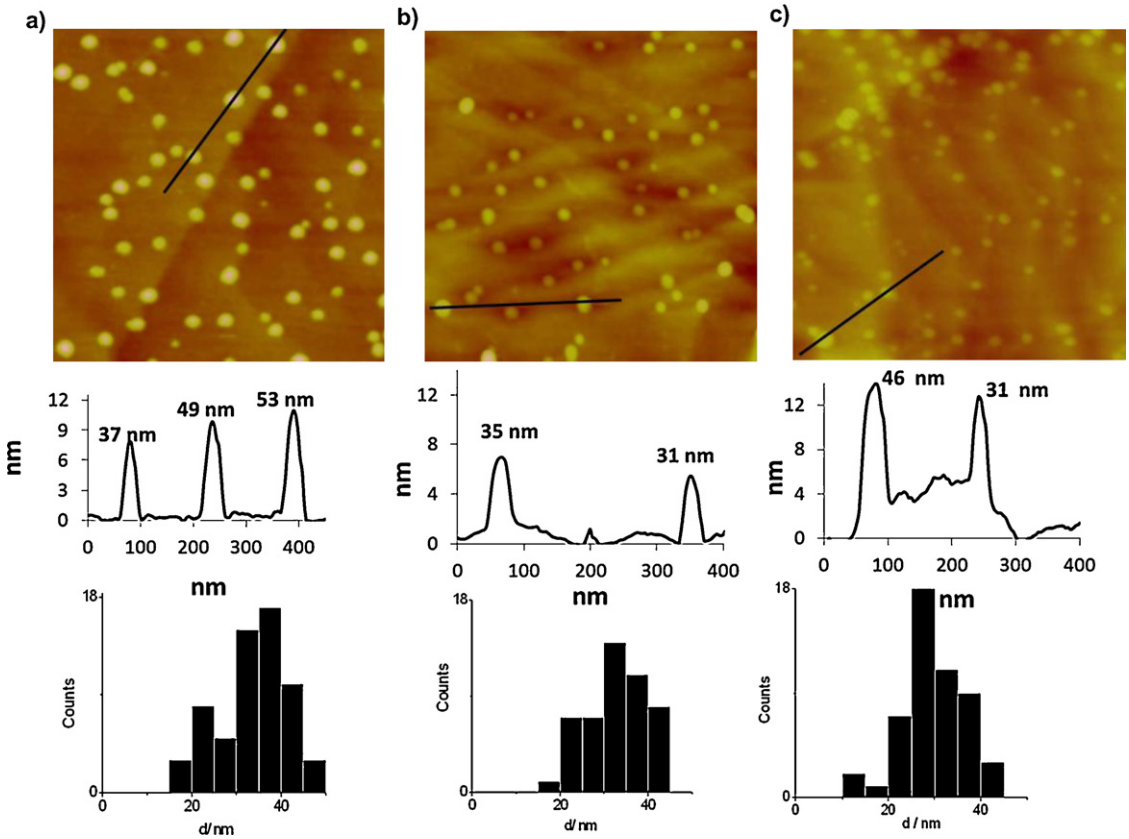

Fig. 5. AFM images (750 mm × 750 nm) of modified gold electrodes with (a) AuNPs/CS_2/epinephrine (ethanol, $z = 20$ nm), and AuNPs/CS_2/tryptophan from (b) ethanol, $z = 20$ nm and (c) aqueous, $z = 42$ nm solutions. AFM profiles and size distribution histograms are displayed below each image.

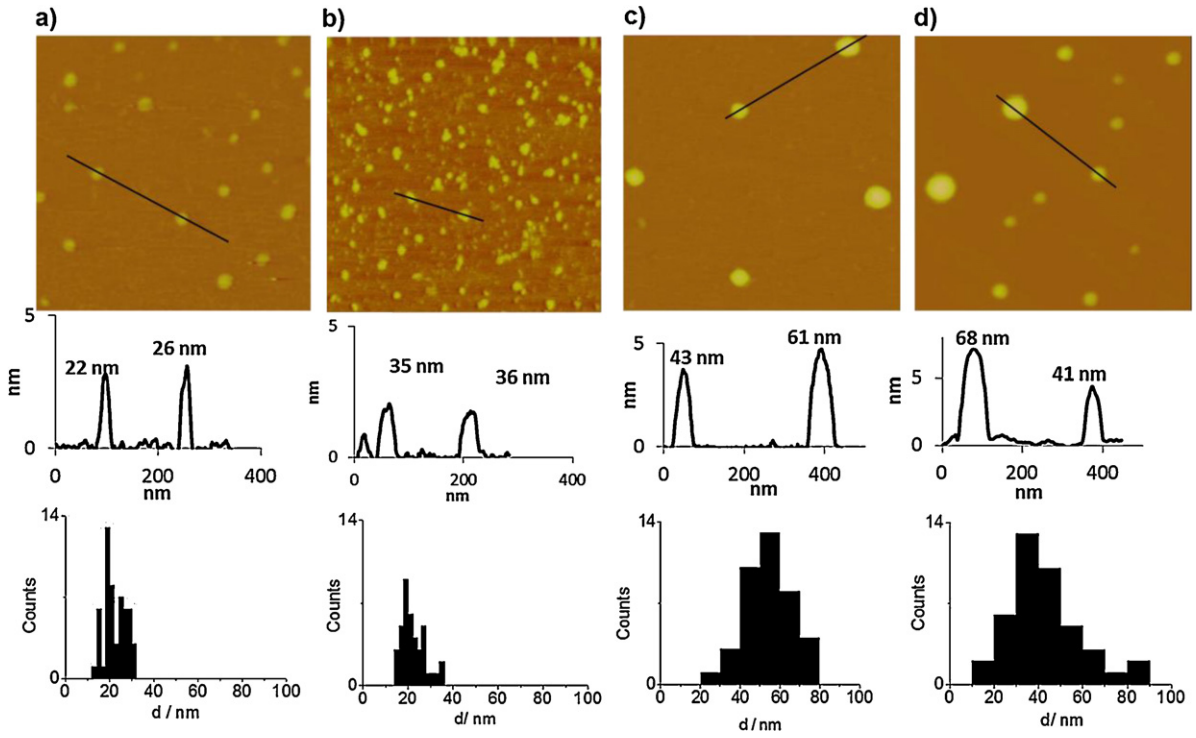

Fig. 6. AFM topographic images (750 nm × 750 nm; z = 15 nm) of mica after drop casting of AuNPs/citrate before (a) and after reaction with: CS_2 (b), CS_2 and epinephrine (c) and CS_2 and tryptophan (d). AFM profiles and size distribution histograms are displayed below each image.

means, for instance, that the excess of epinephrine molecules in solution do not interact with adsorbed CS_2 to form more dithiocarbamates.

3.2. One-step immobilization of glucose oxidase-functionalized AuNPs

Glucose oxidase has been chosen to prove that biomolecules, that possess a large number of aminoacids, can be also immobilized through the one-pot reaction with CS_2 in the presence of nanoparticles. Fig. 7a shows the electrochemical responses of modified Au(1 1 1) surface with only CS_2, CS_2/glucose oxidase, CS_2/AuNPs and also with CS_2/AuNPs/glucose oxidase in PBS solution, containing 0.1 mM ferrocenedicarboxylic acid and 0.50 mM glucose. The enzymatic catalytic mechanism of glucose oxidase toward glucose, using ferrocene derivatives as electron-mediators is well known and widely reported [14,43–45]. The cyclic voltammogram obtained for CS_2 SAM on Au (1 1 1) exhibits a reversible redox process with $E_{1/2}$ = 0.40 V with a ΔE_p = 70 mV at a scan rate of 5 mV s^{-1}, assigned to the ferrocenedicarboxylic oxidation/reduction process. When the Au(1 1 1) is modified with CS_2 and AuNPs, the electrochemical signal increases, probably due to the larger surface area available for soluble ferrocene to be electrochemically oxidized and reduced. A catalytic response with a similar oxidation current increase is observed for the gold surface exposed to CS_2 and glucose oxidase. However, the greatest change in the electrochemical signal of ferrocene mediator is observed for Au(1 1 1) modified with AuNPs/CS_2/glucose oxidase. A significant increase of the oxidation peak of mediator regarding its reduction counterpart was developed as a consequence of the enzymatic oxidation of glucose by GOx, revealing the successful immobilization of the enzyme on the surface of the electrode.

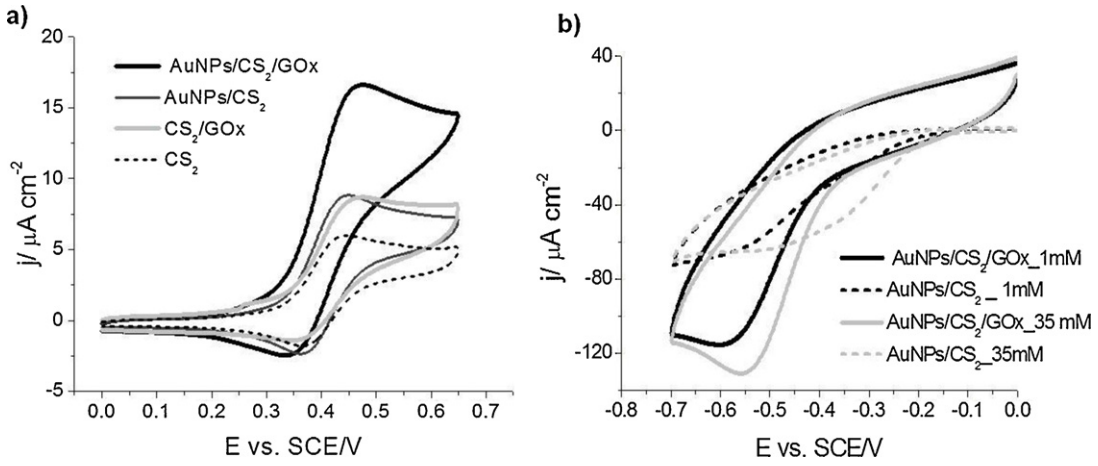

Fig. 7. Cyclic voltammograms of modified electrodes (a) in 0.1 mM ferrocenedicarboxylic acid in PBS solution containing 0.50 mM glucose, at 5 mV s^{-1} and (b) CS_2/AuNPs and AuNPs/CS_2/GOx in PBS containing 1 and 35 mM of glucose, at 50 mV s^{-1}.

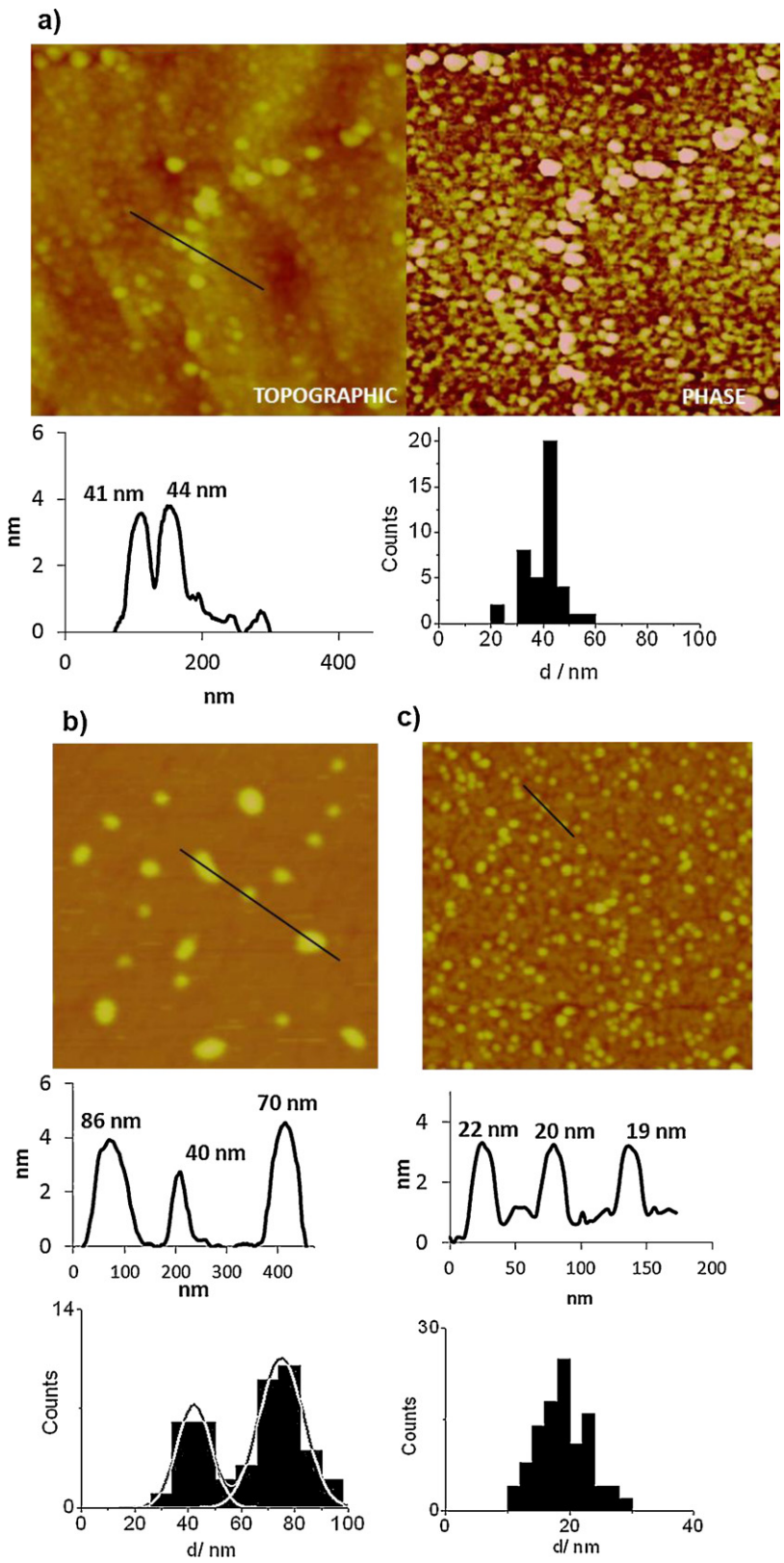

Fig. 8. AFM images (750 nm × 750 nm) of (a) modified gold electrodes with AuNPs/CS_2/GOx; $z_{topography}$ = 15 nm; z_{phase} = 40°; and of mica upon drop casting of AuNPs modified with glucose oxidase (z = 15 nm) in the presence (b) and absence (c) of CS_2. AFM profiles and size distribution histograms are displayed below each image. The histogram in Fig. 8b was fitted with a bimodal Gaussian distribution.

The biological activity of the modified electrodes with AuNPs and GOx toward the oxidation of glucose was also tested by following the reduction of H_2O_2 formed during the catalytic reaction in the absence of a redox mediator. Fig. 7b shows the cyclic voltammograms obtained for gold modified with AuNPs/CS_2 and AuNPs/CS_2/GOx in a PBS solution saturated with O_2, in the presence of 1 and 35 mM of glucose. There is an increase of the cathodic process intensity at ca. −0.550 V vs. SCE, assigned to the reduction of H_2O_2 [46], when the glucose concentration increases from 1 to 35 mM. In the absence of GOx, for both glucose concentrations studied, this reduction process could not be detected. Thus, confirming that glucose oxidase is still active upon one-step immobilization on gold surface.

AFM topographic and phase imaging of the modified electrodes with AuNPs/CS_2/glucose oxidase are presented in Fig. 8a. It is possible to observe that flat Au(1 1 1) electrodes are covered by small granular features of ca. 20 nm which are attributed to adsorbed enzymes via CS_2 on the surface. In addition, larger globules with ca. 40 ± 6 nm, exhibiting a higher contrast in the phase imaging, are assigned to bio-functionalized AuNPs with glucose oxidase, supporting the one-step functionalization of AuNPs and adsorption on gold surface. Fig. 8b and c corresponds to AFM images of mica with casted AuNPs modified with glucose oxidase in the presence and absence of CS_2, from PBS solutions, respectively. The bio-functionalization of AuNPs with CS_2/GOx (Fig. 8b) in aqueous solutions is supported by the increase of the size of AuNPs, where some large aggregates with distinct shapes can be clearly depicted (histogram fitted to a bimodal Gaussian distribution with two maximum at 42 and 75 nm), as well as by a slight shift of the plasmon resonance band wavelength to 530 nm (Fig. S3, Supplementary Materials). It is noteworthy to observe, that in the absence of CS_2, gold nanoparticles have similar diameters to the pristine AuNPs/citrate (Fig. 8c), indicating that this small molecule plays crucial role in the bio-functionalization process.

In similarity with the previously discussed in Section 3.1, modified AuNPs with GOx on gold electrodes present smaller diameters and less irregular shaped particles than those observed on mica shown in Fig. 8b, that should be a consequence of AuNPs adsorption onto Au(1 1 1).

4. Conclusions

It was demonstrated that both epinephrine, a secondary amine, and tryptophan could be successfully immobilized together with AuNPs on a flat gold electrode, using a one-pot reaction with CS_2. A significant increase in the amount of immobilized epinephrine and the aminoacid due to the presence of AuNPs is achieved when the reaction is prepared either from ethanolic or aqueous solutions. The addition of nanoparticles has revealed to be particularly relevant to increase the coverage of the aminoacid prepared from aqueous solutions, as confirmed by the redox studies in acidic medium and also through the total amount of sulfur atoms reductively desorbed from the electrode surface.

XPS analysis of modified gold with AuNPs/CS_2/epinephrine, CS_2/epinephrine and AuNPs/CS_2 reveal only one ionization in the S2p region, assigned to sulfur–metal bond. Ionizations at higher binding energies typical of free unbound sulfur species were not detected in any sample.

The bioactivity of modified electrodes with glucose oxidase through CS_2, together with AuNPs on flat Au(1 1 1), has been attested toward the oxidation of glucose. For the same amount of substrate the oxidation current of the redox mediator (ferrocenedicarboxilic acid) is greatly increased when the enzyme is attached to the nanostructured electrode. Furthermore, it was possible to detect in a saturated O_2 solution, the reduction peak of H_2O_2, which increases with glucose concentration, formed during the catalytic reaction, demonstrating that immobilized GOx preserve its biological activity. The morphological characterization of the electrodes by AFM supported the feasibility of this simple methodology, where the modified AuNPs, with increased diameters regarding pristine citrate stabilized AuNPs appeared distributed on the electrode surface.

The data here reported shows the potential applications of this simple procedure to the preparation of electrochemical and/or optical biosensing surface from aqueous solutions. Optimization studies (e.g. effect of pH, surfactant addition, AuNPs concentration) will be carried on to further increase the amount of surface confined bio-functionalized AuNPs.

Acknowledgement

The authors acknowledge to FCT for financial support: PhD scholarship, SFRH/BD/70673/2010, PTDC/QUI/66612/2006, PEst-OE/QUI/UI0612/2011 and Programme Ciência 2007.

Appendix A. Supplementary data

Supplementary data associated with this article can be found, in the online version, at http://dx.doi.org/10.1016/j.electacta.2012.08.021.

References

[1] R.F. Taylor, J.S. Schultz (Eds.), Handbook of Chem. Biol. Sensors, Institute of Physics Pub., Philadelphia, 1996.
[2] S. Ko, T.J. Park, H.-S. Kim, J.-H. Kim, Y.-J. Cho, Biosensors and Bioelectronics 24 (2009) 2592.
[3] H. Wang, J. Wu, J. Li, Y. Ding, G. Shen, R. Yu, Biosensors and Bioelectronics 20 (2005) 2210.
[4] J. Pendry, Science 285 (1999) 1687.
[5] S.D. Hudson, H.-T. Jung, V. Percec, W.-D. Johansson, G. Cho, K. Balagurusamy, Science 278 (1997) 449.
[6] K. Svoboda, S.M. Block, Optics Letters 19 (1994) 930.
[7] M.J. Feldstein, C.D. Keating, Y.-H. Liau, M.J. Natan, N.F. Scherer, Journal of the American Chemical Society 119 (1997) 6638.
[8] K. Fukumi, A. Chayahara, K. Kadono, T. Sakaguchi, Y. Horino, M. Miya, K. Fujii, J. Hayakawa, M.J. Satou, Journal of Applied Physics 75 (1994) 3075.
[9] R.F. Hagland, L. Yang, R.H. Magruder, J.E. Wittig, K. Becker, R.A. Zuhr, Optics Letters 18 (1993) 373.
[10] B.-W. Park, D.-S. Kim, D.-Y. Yoon, Korean Journal of Chemical Engineering 28 (2011) 64.
[11] P. Pandey, S.P. Singh, S.K. Arya, V. Gupta, M. Datta, S. Singh, B.D. Malhotra, Langmuir 23 (2007) 3333.
[12] B. Zheng, S. Xie, L. Qian, H. Yuan, D. Xiao, M.M.F. Choi, Sensors and Actuators B: Chemistry 152 (2011) 49.
[13] A.-L. Morela, R.-M. Volmanta, C. Méthiviera, J.-M. Krafft, S. Boujdaya, C.-M. Pradiera, Colloids and Surfaces B 81 (2010) 304.
[14] I. Almeida, A.C. Cascalheira, A.S. Viana, Electrochimica Acta 55 (2010) 8686.
[15] Y. Zhao, W. Pérez-Segarra, Q. Shi, A. Wei, Journal of the American Chemical Society 127 (2005) 7328.
[16] A.L. Eckermann, J.A. Shaw, T.J. Meade, Langmuir 26 (2010) 2904.
[17] H. Zhu, D.M. Coleman, C.J. Dehen, I.M. Geisler, D. Zemlyanov, J. Chmielewski, G.J. Simpson, A. Wei, Langmuir 24 (2008) 8660.
[18] R. Cao, A. Díaz Jr., R. Cao, A. Otero, R. Cea, M.C. Rodríguez-Arguëlles, C. Serra, Journal of the American Chemical Society 129 (2007) 6927.
[19] P. Morf, F. Raimondi, H.-G. Nothofer, B. Schnyder, A. Yasuda, J.M. Wessels, T.A. Jung, Langmuir 22 (2006) 658.
[20] R.D. Weinstein, J. Richards, Langmuir 23 (2007) 2887.
[21] K. Chen, H.D. Robinson, Journal of Nanoparticle Research (2011) 13751.
[22] S.K. Kailasa, H.-F. Wu, Analyst 137 (2012) 1629.
[23] M. Li, F. Gao, P. Yang, L. Wang, B. Fang, Surface Science 602 (2008) 151.
[24] J.F. Cabrita, A.S. Viana, C. Eberle, F.-P. Montforts, A. Mourato, L.M. Abrantes, Surface Science 603 (2009) 2458.
[25] J. Turkevich, P.C. Stevenson, J. Hiller, Discussions of the Faraday Society 11 (1951) 55.
[26] J. Kimling, M. Maier, B. Okenve, V. Kotaidis, H. Ballot, A. Plech, Journal of Physical Chemistry B 110 (2006) 15700.
[27] V.C. Ferreira, A.F. Silva, L.M. Abrantes, Journal of Physical Chemistry C 114 (2010) 7710.
[28] W. Haiss, N.T.K. Thanh, J. Aveyard, D.G. Fernig, Analytical Chemistry 79 (2007) 4215.
[29] S.-M. Chen, J.-Y. Chen, V.S. Vasantha, Electrochimica Acta 52 (2006) 455.

[30] K.-J. Huanga, C.-X. Xu, W.-Z. Xie, W. Wang, Colloids and Surfaces B 74 (2009) 167.
[31] N.T. Nguyen, Z. Monika, G. Wrona, Dryhurst, Journal of Electroanalytical Chemistry 199 (1986) 101.
[32] N.C. Guo, Z.Z. Feng, W. Xiu Li, D.J. Ping, C.H. Qin, Analytica Chimica Acta 452 (2002) 245.
[33] G. Jin, X.-Q. Lin, Electrochemistry Communications 6 (2004) 454.
[34] Z.H. Wang, A.S. Viana, G. Jin, L.M. Abrantes, Bioelectrochemistry 69 (2006) 180.
[35] A. Ulman, Chemical Reviews 96 (1996) 1533.
[36] O.C. Monteiro, A.C.C. Esteves, T. Trindade, Chemistry of Materials 14 (2002) 2900.
[37] F.P. Cometto, C.A. Calderón, E.M. Euti, D.K. Jacquelín, M.A. Pérez, E.M. Patrito, V.A. Macagno, Journal of Electroanalytical Chemistry 661 (2011) 90.
[38] O. Cavalleri, G. Gonella, S. Terreni, M. Vignolo, P. Pelori, L. Floreano, A. Morgante, M. Canepa, R. Rolandi, Journal of Physics: Condensed Matter 16 (2004) S2477.
[39] M.-C. Bourg, A. Badia, R.B. Lennox, Journal of Physical Chemistry B 104 (2000) 6562.
[40] F.V. Wrochem, F. Scholz, A. Schreiber, H.-G. Nothofer, W.E. Ford, P. Morf, T. Jung, A. Yasuda, J.M. Wessels, Langmuir 24 (2008) 6910.
[41] S. Ramsaywack, S. Martić, S. Milton, L. Gates, A.S. Grant, M. Labib, A. Decken, H.-B. Kraatz, Journal of Physical Chemistry C 116 (2012) 7886.
[42] N. Graf, E. Yegen, T. Gross, A. Lippitz, W. Weigel, S. Krakert, A. Terfort, W.E.S. Unger, Surface Science 603 (2009) 2849.
[43] S. Zhang, N. Wang, Y. Niu, C. Sun, Sensors and Actuators B: Chemistry 109 (2005) 367.
[44] S. Zhao, K. Zhang, Y. Bai, W. Yang, C. Sun, Bioelectrochemistry 69 (2006) 158.
[45] S. Zhang, N. Wang, H. Yu, Y. Niu, C. Sun, Bioelectrochemistry 67 (2005) 15.
[46] W. Lu, Y. Luo, G. Chang, X. Sun, Biosensors and Bioelectronics 26 (2011) 4791.